REVIEW ARTICLE

The impact of carbon dioxide removal on temperature parameters over West Africa

E. K. Uzoma[1] · M. O. Adeniyi[1] · D. P. Keller[2] · R. Séférian[3] · E. O. Oladiran[1]

Abstract
Removal of atmospheric carbon dioxide is being considered a suitable option for reducing the recent global rise in atmospheric temperature. The impact of the removal on some climate parameters—near-surface air temperature (TAS), maximum near-surface air temperature (TASMAX), minimum near-surface air temperature (TASMIN) and surface temperature (TS) over West Africa was assessed in this paper. We used CNRM-ESM1-C1 model simulation output consisting of $1\%yr^{-1}$ CO_2 removal from the atmosphere which was compared with CRU observational dataset. Four climatological periods 1990–2019 (reference period), 2040–2069, 2070–2099 and 2100–2129 were considered, and hence the impacts levels in each of the two West African regions, Sahel and Guinea, were estimated in each period with respect to the reference period. The comparison with CRU demonstrated that CNRM-ESM1-C1 model captured temperature variations within major locations in Mauritania, Mali, Niger, Burkina Faso and Senegal with an indication of an underestimation of temperature at locations above 18° N. The value of each parameter was projected to decrease progressively the periods and much impacts were also projected in the last period for the two regions. Time of retreat to 2 °C reduction target is projected a decade before the year 2100 and will occur earlier with greater impact in the Guinea region than in Sahel region. The root mean square deviation of each ensemble member was found at RMSD < 0.5 with respect to the model ensemble mean per parameter, although RMSD > 0.5 was found with GFDL-ESM4 model for TAS and TS.

✉ E. K. Uzoma
uzomaechefulachik@gmail.com

M. O. Adeniyi
mojisolaadeniyi@yahoo.com

D. P. Keller
dkeller@geomar.de

R. Séférian
rseferian.cnrm@gmail.com

E. O. Oladiran
oluyemi_oladiran@yahoo.co.uk

[1] Department of Physics, University of Ibadan, Ibadan, Nigeria

[2] GEOMAR Helmholtz Centre for Ocean Research Kiel, Kiel, Germany

[3] Centre National de Recherches Météorologiques, Toulouse, France

1 Introduction

Efforts to reduce the concentration of carbon dioxide in the atmosphere are being made by most world bodies in a bid to tackle the menace of climate change. The Paris Agreement on climate change is targeted at ensuring that the surface temperature increase does not go beyond 2 °C with respect to its global mean preindustrial (1850–1900) level (UNFCCC 2015). According to Miranda et al. (2017), carbon dioxide removal comprises a set of options for actively removing carbon dioxide from the atmosphere to limit global warming and its effects. By reducing the greenhouse effect, which leads to cooling, carbon dioxide removal (CDR) also triggers climate–carbon cycle feedbacks (Keller et al. 2018). Together, these responses affect the efficacy of CDR and mean that removing 1Gt of CO_2 from the atmosphere will not ultimately reduce the atmospheric CO_2 concentration by 1 Gt in the short run (Keller et al. 2018).

Emission reduction options are adopted to tackle global warming caused by greenhouse gases. These options include alternative source of energy or renewable energy sources, alternative means of transport such as bicycling, use of

hybrid cars and the implementation of carbon price policy. Climate change mitigation scenarios are now integrated with carbon dioxide removal options in consonance with the Paris Agreement goals (Clarke et al. 2014; van Vuuren et al. 2013; Fuss et al. 2014).

Afforestation and reforestation options are considered to have great potential in carbon dioxide removal on a global scale. A significant impact ranging from 4 to 12 Gt CO_2 per year is estimated globally (Smith et al. 2016). According to Griscom et al. (2017), the capacity estimate for afforestation and reforestation stands at 28 Gt CO_2 per year. An estimate between 1.8 and 3.3 Gt CO_2 per year has been made as carbon dioxide removal potential for biochar options (Woolf et al. 2010). Wetlands are another carbon dioxide removal option. Zedler and Kercher (2005) revealed that about 44–71% of the world's terrestrial biological carbon pool are stored up in peatlands and coastal wetlands. Proposals on accelerated weathering option are also being considered. By this, a huge chunk of carbon dioxide can be drawn from the air and bound permanently (Lackner et al. 1995; Chiang and Pan 2017).

Technically, direct air capture option has the potential above 20 Gt CO_2 per year, but a significant amount of between 2 and 5 Gt CO_2 should actually be expected per year with global deployment (USNAS 2015). Carbon sequestration of about hundreds of billions to trillions of tons can also be achieved through ocean alkalinity enhancement CO_2 removal option (Renforth and Henderson 2017). An estimate of 2–8 Gt CO_2 per year of carbon dioxide removal can be achieved with the biomass energy with carbon capture and storage (BECCS) option by 2050 (Kemper 2015; McLaren 2012; USNAS 2015).

By Keller et al. (2018), CDR options have the potential to achieve the target of CO_2 removal from the atmosphere, but the seeming drawbacks are (i) the slow acting of the methods and the long actualization time for full development and deployment at climatically relevant scales–that is, decades to centuries are needed before atmospheric CO_2 can be reduced to some level of interest, (ii) the immaturity of the few methods in terms of technology, which have the theoretical potential to rapidly remove more carbon dioxide. African forests, which are predominantly in equatorial countries, are currently carbon sinks. On balance, these forests remove about 1.1 gigatons of carbon dioxide from the atmosphere annually (Harris et al. 2021).

Climate projections over Africa for the twenty-first century reveal that its land temperature will rise faster than the global mean temperature, particularly in the more arid regions (Niang et al. 2015). The increasing trend in temperature over West Africa under low, intermediate and very high emission scenarios were projected to be 0.04 °C decade^{-1}, 0.24 °C decade^{-1} and 0.6 °C decade^{-1}, respectively, with projected warming values of 1.2 (1.3) °C, 1.4 (2.4) °C and

1.7 (4.2) °C, respectively, for the near (long)-term period. The projection of rising temperatures divides West Africa into two zones. First, is the north of 12.5°N where the temperature difference is 2 °C for the first 30 years, reaching some 2.5 °C toward the end of the twenty-first century. Second, is the south of 12.5°N where the temperature difference is 1 °C during the period 2011–2040 and then reaches 2 °C in 2071–2100 (Deme et al. 2017). In the same vein, Almazroui et al. (2020) projected a continuous warming over West Africa during the twenty-first century.

Temperature projections over West Africa for the end of the twenty-first century (year 2100) from both the CMIP3 GCMs (SRES A2 and A1B scenarios) and CMIP5 GCMs (RCP4.5 and RCP8.5 scenarios) range between 3 °C and 6 °C above the late twentieth century baseline (Meehl et al. 2007; Fontaine et al. 2011; Diallo et al. 2012; Monerie et al. 2012). Regional downscalings produce a similar range of projected change (Patricola and Cook 2010, 2011; Mariotti et al. 2011; Vizy et al. 2013). Sahel and tropical West Africa were identified by Diffenbaugh and Giorgi (2012) as hotspots of climate change for both RCP4.5 and RCP8.5 pathways, while Mora et al., (2013) projected unprecedented climates to occur earliest (late 2030s to early 2040s) in these regions. Since both RCP4.5 and RCP8.5 are emission scenarios representing medium stabilization and a high baseline emission scenarios respectively, it is obvious that the levels of impacts stated above (that is, between 3 °C and 6 °C) are expected over West Africa by the year 2100 without carbon dioxide removal.

According to Niang et al. (2014), temperatures over West Africa have increased over the last 50 years in line with an increase in global temperatures; near-surface temperatures (TAS) over West Africa and the Sahel have increased within this period of years. The Earth's average surface temperature has already warmed by 1.09 °C since preindustrial times (1850–1900). However, West Africa's climate has warmed even more than the global average in the past few decades (IPCC 2021).

It has been scientifically established that global warming is as a result of enhanced anthropogenic greenhouse gases (GHGs) forcing on global climate (IPCC 2013), of which carbon dioxide is a major contributor. MacDougall (2013) used the University of Victoria Earth system-climate model to study "reversing climate warming by artificial atmospheric carbon-dioxide removal". The result showed that artificially removing CO_2 from the atmosphere will lead to a return to a "safe" CO_2 concentration within this millennium. In Switzerland, direct air capture has been used to remove about 900 tons of CO_2 annually (Marshall 2017). Borchers et al. (2022), in their work on "Scoping carbon dioxide removal options for Germany" found that CDR could provide sufficient potential to counterbalance the residual emissions. According to CRS (2022), carbon capture and

sequestration in the USA was found to have the capacity to remove approximately 4717 metric tons of CO_2 per day.

However, the study of the impacts of carbon dioxide removal on the climate over West Africa is yet to receive widespread attention. This paper is therefore targeted at assessing the impacts of the removal of carbon dioxide from the atmosphere on some temperature parameters—surface temperature, near-surface air temperature, maximum near-surface air temperature and minimum near-surface air temperature over West Africa and investigating the possible time of retreat to 2 °C level of reduction target.

2 Methodology

2.1 Area of study

West Africa is a 16-country region of Africa, 7,924,596 km^2 in area and composed of a broad band of semi-arid terrain known as Western Sudan on the northern portion with Atlantic Ocean on the west. It borders Sahara Desert on the north and the Guinea Coast forests toward the southern part. Within the north is a transitional zone known as Sahel, while the south constitutes the Savanna grassland. While the northern part receives an average rainfall of 250 mm, the south receives an average of 1250 mm of rainfall. Typical daily maximum temperature values over the Guinea Savanna range from 26 to 35 °C, while over the Sahel, temperatures range from about 38–44 °C (Fitzpatrick et al. 2020). Figure 1 represents the map of the study region.

2.2 Observational dataset (CRU 4.04)

The gridded Climatic Research Unit (CRU) Time Series (TS) data version 4.04 data are month-by-month variations in climate over the period 1901–2019, provided on high-resolution (0.5×0.5 degree) grids, produced by CRU at the University of East Anglia, UK (Harris et al. 2020). All CRU output files are actual values and not anomalies. To test the ability of models to represent the historical climate, simulations of that historical past (for the same period as the data available for CRU) are compared against CRU. To evaluate the projected temperature and precipitation, the model's representation of the seasonal cycle (monthly values for key variables) is additionally evaluated with respect to historic values.
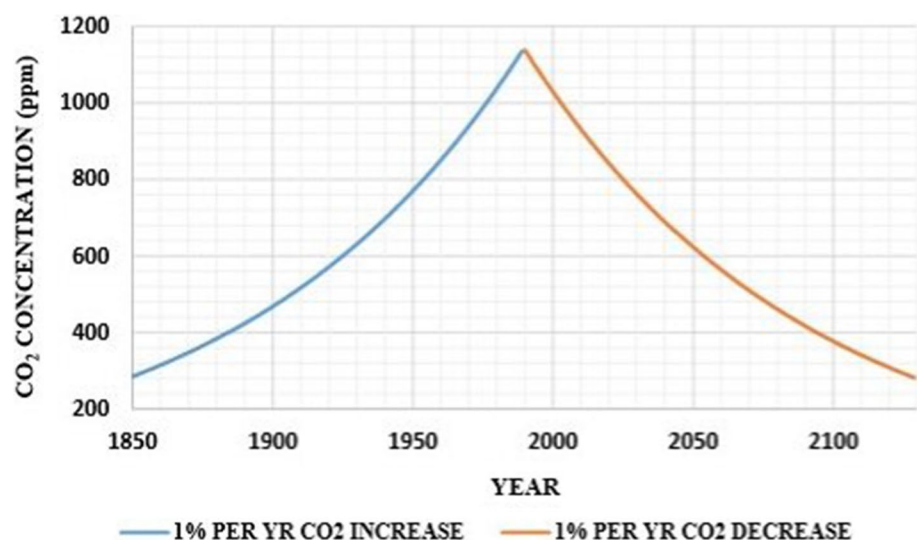
2.3 Experimental protocol

The data used are surface temperature (TS), near-surface air temperature (TAS), minimum near-surface air temperature (TASMIN) and maximum near-surface air temperature

Fig. 1 The map of the study area
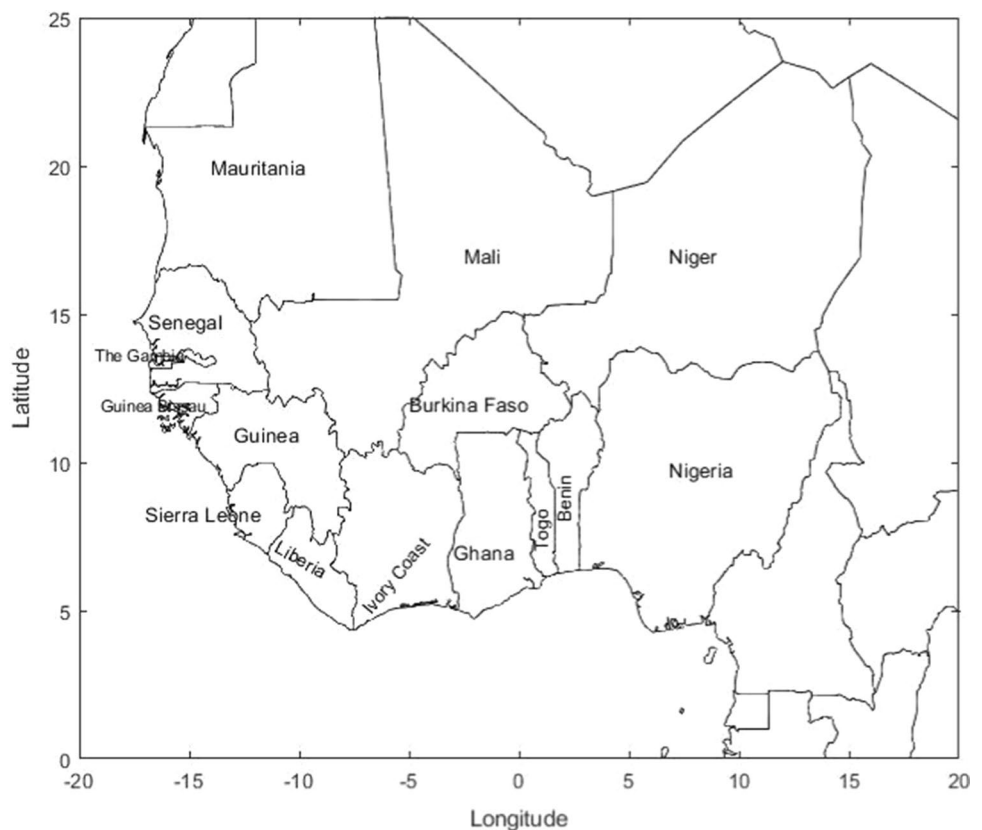
(TASMAX), which are the Centre National de Recherches Meteorologiques, Earth System Model-1 (CNRM-ESM1-C1) simulation outputs acquired from the data archives of Centre National de Recherches Météorologiques. These are monthly C1 experiment data prepared for Carbon Dioxide Removal Model Intercomparison Project (CDRMIP) with 1% per year CO_2 decrease up to preindustrial level (Keller et al. 2018). The C1 experiment investigates the "reversibility" of the climate system by leveraging the prescribed 1% per year CO_2 (1pctCO$_2$) concentration increase experiment that was done for prior CMIPs and is a key run for CMIP6 (Eyring et al. 2016). The 1pctCO$_2$ experiment branches from the DECK piControl experiment, which should ideally represent a near-equilibrium state of the climate system under imposed year 1850 conditions. Starting from year 1850 conditions (piControl global mean atmospheric CO_2 should be 284.7 ppm), the 1pctCO$_2$ simulation prescribes a CO_2 concentration increase at a rate of $1\%yr^{-1}$ (i.e., exponentially). The only externally imposed difference from the piControl experiment is the change in CO_2; i.e., all other forcing is kept at that of year 1850. The simulation of CO_2 increase continues until the CO_2 concentration reaches four times the piControl (1138.8 ppm; a total of 140 years into the run). Now at this point begins a restart of $1\%yr^{-1}$ removal of CO_2 from the atmosphere (start removal at the beginning of the 140th year: 1 January) until the CO_2 concentration reaches 284.7 ppm. Also, as done in the $1\%yr^{-1}$ CO_2 increase, the only externally imposed forcing should be the change in CO_2 (all other forcing is kept at that of year 1850). The CO_2 concentration is then held at 284.7 ppm for as long as possible (a minimum of 60 years is required), with no change in other forcing (Keller et al. 2018). Figure 2 shows the simulated 1% per year carbon dioxide increase (blue curve) and decrease (orange curve) with our interest in this work in 1% per year carbon dioxide decrease up to preindustrial level.

2.4 Statistical analysis

2.4.1 Performance of CNRM-ESM1-C1 model historical dataset with CRU observational dataset

In a bid to determine how well the CNRM-ESM1-C1 model output will perform in making future projections, we first regridded the CRU dataset to the grid size of CNRM-ESM1-C1 historical temperature dataset. This was done using the first order conservative remapping regridding method fit for Earth system modeling framework. The CNRM-ESM1-C1 historical temperature dataset was compared against CRU 4.04 observational temperature dataset within the same period 1990–2019. The mean bias error between the two datasets was calculated and the standard deviation of each of the two data outputs was also compared. Equation 1 was used to estimate the mean bias error (MBE). MBE is a statistical index used to assess the mean difference between two data products and, therefore, widely used to measure the over- and underestimation in data products. MBE was calculated thus:

$$MBE = \sum_{1}^{n} \frac{(X_{s,i} - X_{o,i})}{n}, \tag{1}$$

where $X_{s,I}$ and $X_{o,i}$ refer to ith simulated and observed data respectively, and n is used to represent the number of data. Smaller absolute MBE value indicates a better performance of the model. Figure 3a, b shows the direct plots of CRU observational temperature dataset and CNRM-ESM1-C1 historical temperature dataset for the period 1990–2019, respectively. The mean bias error calculated by comparing the two datasets was plotted as shown in Fig. 3c.

Fig. 2 The plot of 1% per year CO_2 increase and decrease
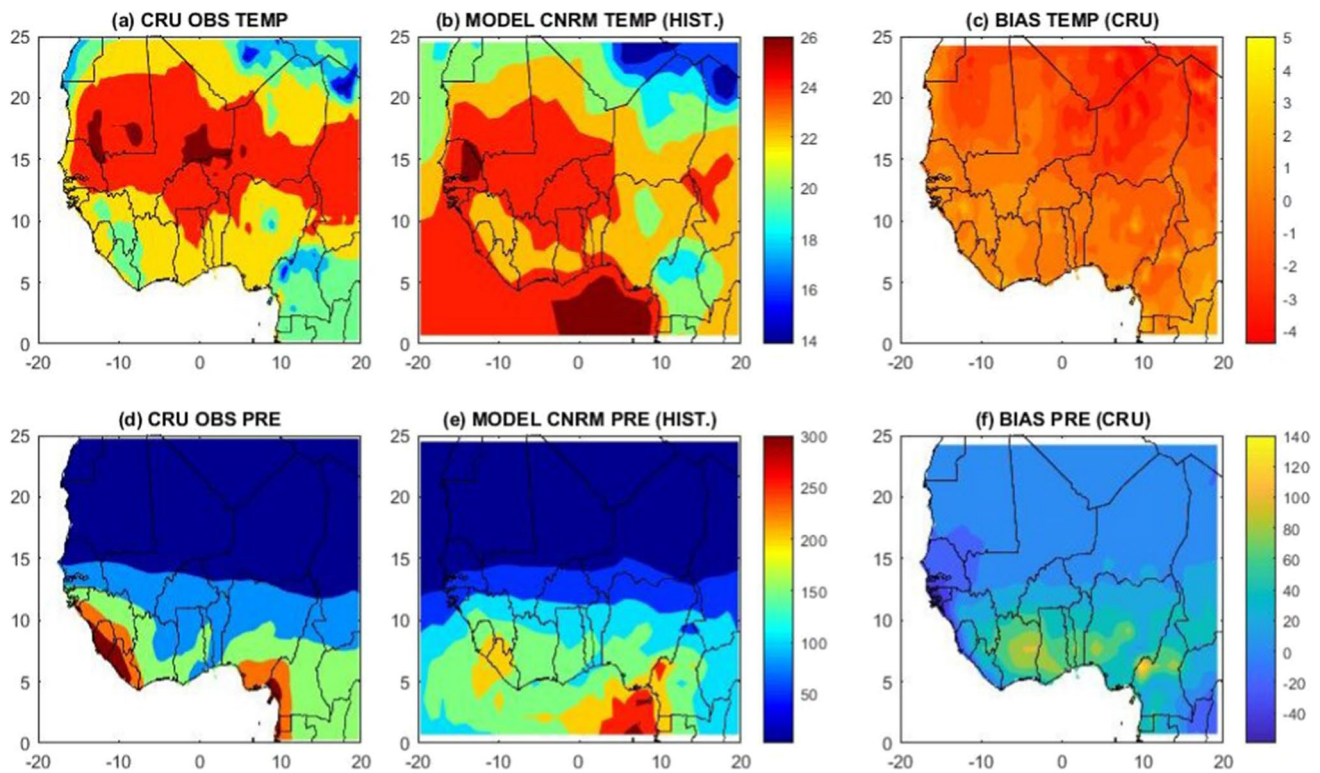
Fig. 3 Comparison between CRU observational dataset and CNRM-ESM1-C1 historical model simulation. **a** (Top left) is the plot of the CRU temperature dataset, **b** (top middle) is the CNRM-ESM1-C1 model historical temperature dataset, **c** (top right) is the bias between **a** and **b**

2.4.2 Analysis of CNRM-ESM1-C1 model simulation output

The CNRM-ESM1-C1 model simulation output over West Africa was extracted from the global output. Two sub-regions—Sahel (latitude 14° N–20° N; longitude 15° W–14° E) and Guinea coast (latitude 6.5° n–10° n; longitude 12° W–10° E), were considered for further analysis. The data were divided into four climatological periods: 1990–2019, 2040–2069, 2070–2099 and 2100–2129. The effect of CDR was assessed by calculating the difference between the reference period (1990–2019) and each of the future periods. The significance of the projected differences or changes was established through Student's t test analysis at 5% statistically significant level (at critical value of 1.96). The maximum and minimum values of the parameters and levels of maximum CO_2 removal impacts in the two regions were also estimated for each of the periods per parameter. The difference between the maximum value of a particular period and that of the reference period gives the CO_2 level of impact for that period (Tables 2 and 3). Time of retreat (ToR) of the temperature to the 2.0 °C reduction target with the deployment of carbon dioxide removal techniques over West Africa was further investigated by considering two of the parameters—TAS and TS—over the Sahel and Guinea coast. The ToR is defined as the year in which the signal- (S)

to-noise (N) ratio, S/N, exceeds particular threshold values (such as − 1 and − 2) expressed using Eq. 2 by Hawkins and Suttons (2011). Each of the parameters was first regressed with its global mean component, assuming that the local climate changes scale with global temperature. Shepard (2019) posited that if the global mean temperature reaches 2 °C of global warming, it will cause significant changes in the occurrence and intensity of temperature extremes in all sub-Saharan regions. West and Central Africa will see particularly large increases in the number of hot days at both 1.5 °C and 2 °C. The regression coefficients, α and β between T_{local} and T_{global}, were estimated according to Eq. 2, with S expressed as

$$S(t) = \alpha T(t) + \beta \tag{2}$$

for each grid point. All estimates were made relative to the reference period 1990–2019. Taking N to be the inter-annual standard deviation of seasonal means, we calculated the signal-to-noise ratio (S/N) for each grid point. The 50th percentile for the grid points having S/N < − 1 and S/N < − 2 was as well estimated in each of the regions (Table 4). By the 50th percentile, we mean a value in the estimated S/N grid points such that almost 50% of the estimated grid points are less than or equal to the value.

2.4.3 Models ensemble mean

The most common approach to characterize multi-model ensemble results is to calculate the arithmetic mean of the individual model results, referred to as an unweighted multi-model mean, which reveals how well each model has fared in objective evaluation (Flato et al. 2013). Hence, the ensemble mean and the ensemble spread (Fig. 3) of different models outputs were estimated based on the available model outputs per temperature parameter and further analyzed according to Ziehmann (2000). Statistically, the consistency of the models requires that the quantity, ensemble consistency (ENC),

$$ENC = \frac{\left\langle \left(o - \bar{f}\right)^2 \right\rangle}{\left\langle \frac{1}{M} \sum_{i=1}^{M} \left(f_i - \bar{f}\right)^2 \right\rangle} - 1 \tag{3}$$

should be equal to $2/(M-1)$. The numerator of (3) is the average squared forecast error of the ensemble mean, while the denominator is the average variance of the ensemble forecasts about the ensemble mean. M is the number of ensemble member models. Values that are larger than $2/(M-1)$ show large bias, whereas lower ones show lower bias in the models. Also, the lower the root mean square deviation (RMSD) of each ensemble member with respect to the ensemble mean, the better is the model performance.

3 Results and discussion

3.1 Model performance with CRU dataset

The result of the validation analysis of the model simulation shows that there are no much variations between the CRU observational dataset and CNRM-ESM1-C1 historical data. The comparison demonstrates that CNRM-ESM1-C1 model captures temperature variations within major locations in Mauritania, Mali, Niger, Burkina Faso and Senegal, although there is an indication of an underestimation of temperature at locations a little above 18° N. These locations are within the Sahel sub-region usually characterized with high temperature. Overestimation of temperature was indicated at Cote D'Ivoire, Liberia and Sierra Leone. Generally, the CNRM-ESM1-C1 model shows relatively good performance across all the locations (Fig. 3c). The standard deviations of 3.3011 and 3.3657 were calculated for CRU observational daraset and the historical model simulation, respectively.

### 3.2 The impacts of CDR protocol on the temperature parameters

The seven-model carbon dioxide reduction ensemble analysis revealed a low deviation of each of the ensemble members from the ensemble mean as can be seen in Fig. 4 and also indicated in Table 1. The CNRM-ESM1-C1 model simulation has the lowest level of spread among the models, which theoretically implies high prediction or simulation accuracy of the models result. The projected changes are statistically significant at the 0.05 level. The projected changes in temperature parameters with respect to the reference period are shown in Figs. 5, 6, 7 and 8 for TAS, TASMAX, TASMIN and TS, respectively. The preindustrial control simulation temperatures are found to be, TAS (22.3 °C), TASMAX (29.8 °C), TASMIN (17.5 °C) and TS (23.2 °C), while the simulated temperature increase for all the parameters at 1% per year CO_2 increase gradually started in the 1870s.

A linear relationship exists between temperature and the concentration of atmospheric carbon dioxide. Reduction in temperature is observed with increased reduction in carbon dioxide concentration as shown in Fig. 9 (also refer to Fig. 2).

TAS shows that for each period, its value was maximum in Mauritania and minimum in Niger. In the period 2040–2069 (Tables 2 and 3), an average level of 1.7 °C reduction is expected in the Sahel and Guinea regions put together with respect to the reference period. It further decreased in the 2070–2099 period and much more in the 2100–2129 period, especially, within the northern part of Mali, Ghana, Togo and Nigeria. There will be also a notable decrease in the values of TAS in the northern part of Mali and Niger in both the 2040–2069 and 2100–2129 periods when compared with the previous period (Fig. 5c and d) and, hence, reduced warming condition will be experienced in these periods.

In Ghana, the near-surface air temperature showed that a warming decrease of 2.8 °C was simulated for the period 2070–2099. Since some health-related issues observed in Ghana are connected to temperature increases, it is expected that the reduction in temperature will make a reasonable impact in the country by minimizing heat-related sicknesses such as cardiovascular diseases, stroke, respiratory and non-communicable diseases, which already affect human life and health in the country. Temperature in West African freshwater bodies was reported in IPCC AR6 (2021) to have risen by 0.1–0.4 °C per decade and by up to 0.6 °C in lake Volta in Ghana. This simulated decrease, however, suggests that the freshwater ecosystem, particularly, in Ghana will be positively impacted with atmospheric carbon dioxide removal. Increases in temperature, among other factors, alter the physical and chemical properties of inland water bodies, affecting water quality and productivity of algae, invertebrates and fish (IPCC 2021). On the contrary, the projected decrease and moderate temperatures under atmospheric carbon dioxide removal will culminate in an enhanced productivity of these organisms.
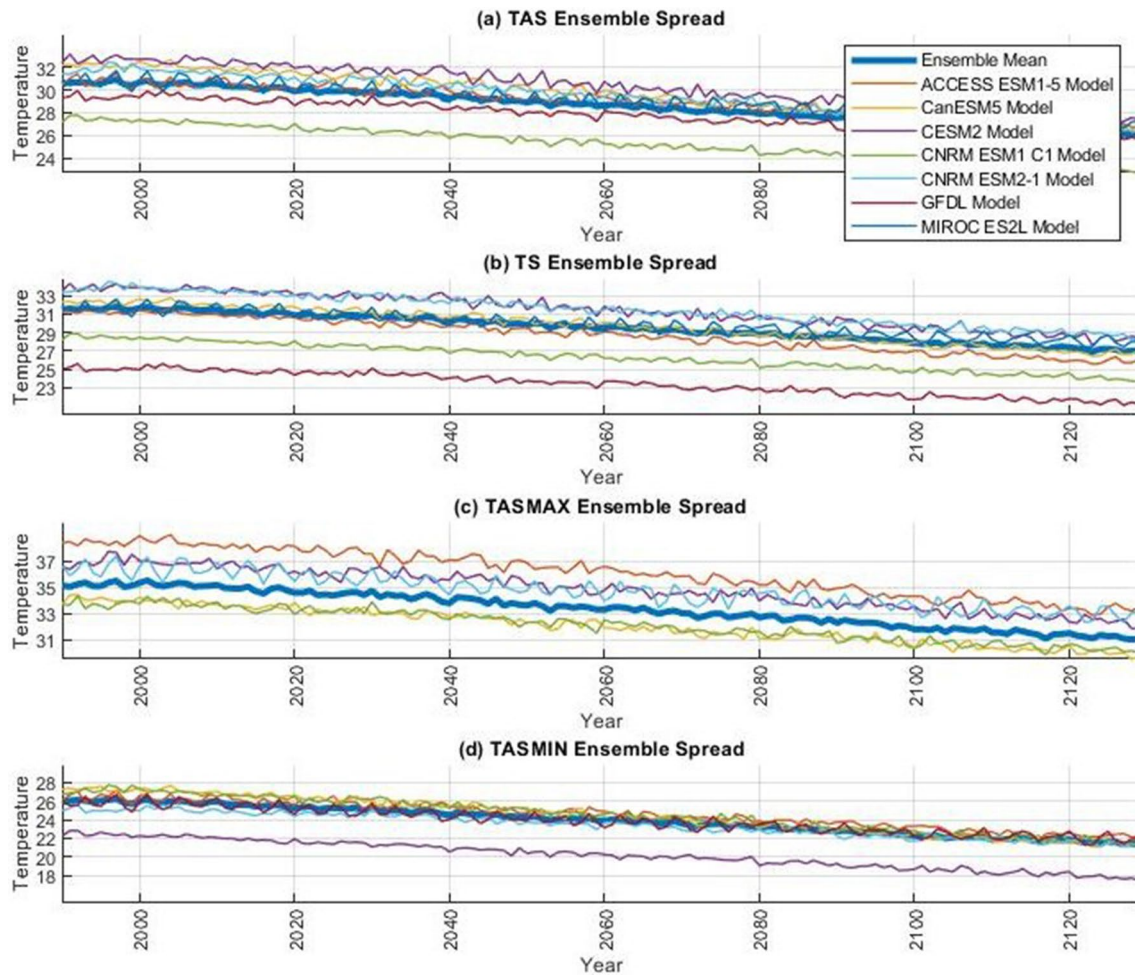
Fig. 4 The seven-model carbon dioxide reduction ensemble spread

**Table 1** Deviation of each ensemble member from the ensemble mean

Variables	Periods	CanESM5	CNRM-ESM1-C1	CNRM-ESM2	GFDL ESM4	MIROC ES2L	ACCESS ESM1	CESM2
TAS	1990–2019	0.3781	0.0024	0.1303	0.4688	0.3500	0.3986	0.3986
	2040–2069	0.4845	0.0048	0.1636	0.6033	0.1902	0.2854	0.2854
	2070–2099	0.4543	0.0480	0.1170	0.5326	0.2251	0.3596	0.3596
	2100–2129	0.5104	0.0044	0.0660	0.5566	0.2932	0.3642	0.3642
TS	1990–2019	0.1676	0.0007	0.2042	0.5853	0.5607	0.4144	0.0326
	2040–2069	0.2791	0.0026	0.2236	0.7095	0.3909	0.2923	0.1665
	2070–2099	0.2360	0.0028	0.1724	0.6320	0.4531	0.3833	0.1687
	2100–2129	0.2787	0.0022	0.1073	0.6459	0.5143	0.3908	0.1740
TASMIN	1990–2019	0.0352	0.0072	0.2106	0.2845	0.5440	0.7183	N/A
	2040–2069	0.1358	0.0055	0.1872	0.3928	0.3740	0.6745	N/A
	2070–2099	0.0817	0.0060	0.2560	0.3198	0.4382	0.7867	N/A
	2100–2129	0.1304	0.0065	0.3251	0.3624	0.4865	0.7780	N/A
TASMAX	1990–2019	0.4083	0.0074	0.0869	0.1545	0.4532	N/A	N/A
	2040–2069	0.5034	0.0088	0.0627	0.2996	0.2975	N/A	N/A
	2070–2099	0.4938	0.0091	0.0960	0.2415	0.3354	N/A	N/A
	2100–2129	0.5236	0.0077	0.1709	0.2269	0.4398	N/A	N/A

N/A indicates that the models data for the variables TASMIN and TASMAX were not available

Fig. 5 The difference between the reference period 1990–2019 of TAS and the periods 2040–2069, 2070–2099 and 2100–2129 under 1% per year CO_2 decrease up to preindustrial level. **a** Shows the reference period. **b–d** Show the projected differences, statistically significant at 5% level and represented by the long color bar
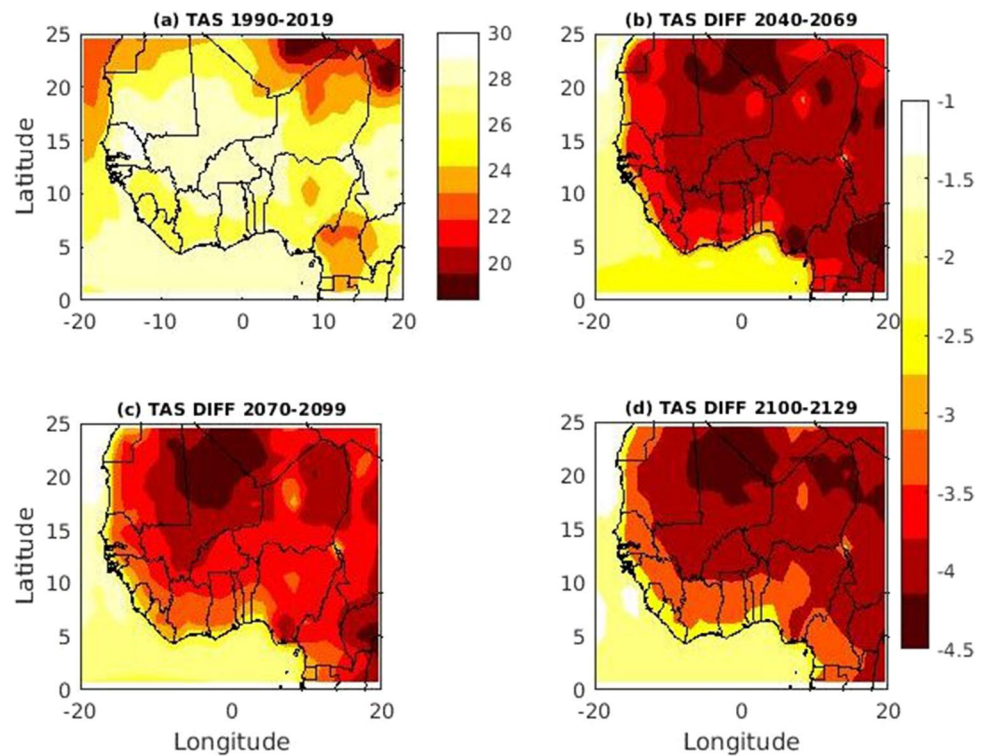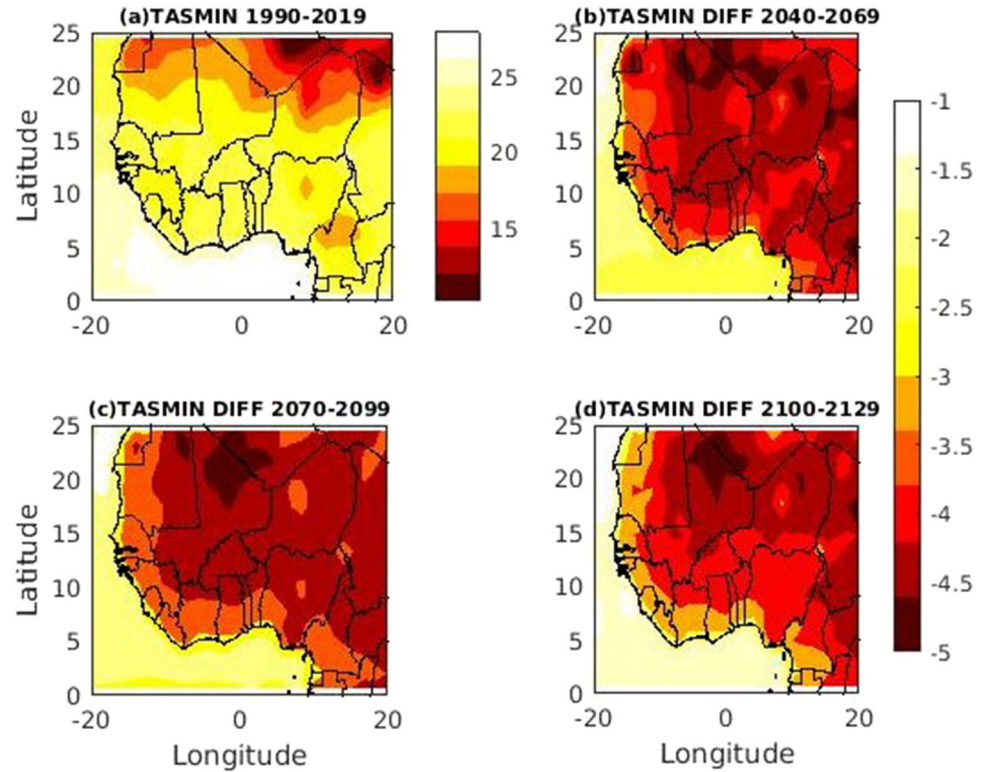
Fig. 6 The difference between the reference period (1990–2019) of TASMAX and the periods 2040–2069, 2070–2099 and 2100–2129 under 1% per year CO_2 decrease up to preindustrial level. **a** Shows the reference period. **b–d** Show the projected differences, statistically significant at 5% level and represented by the long color bar
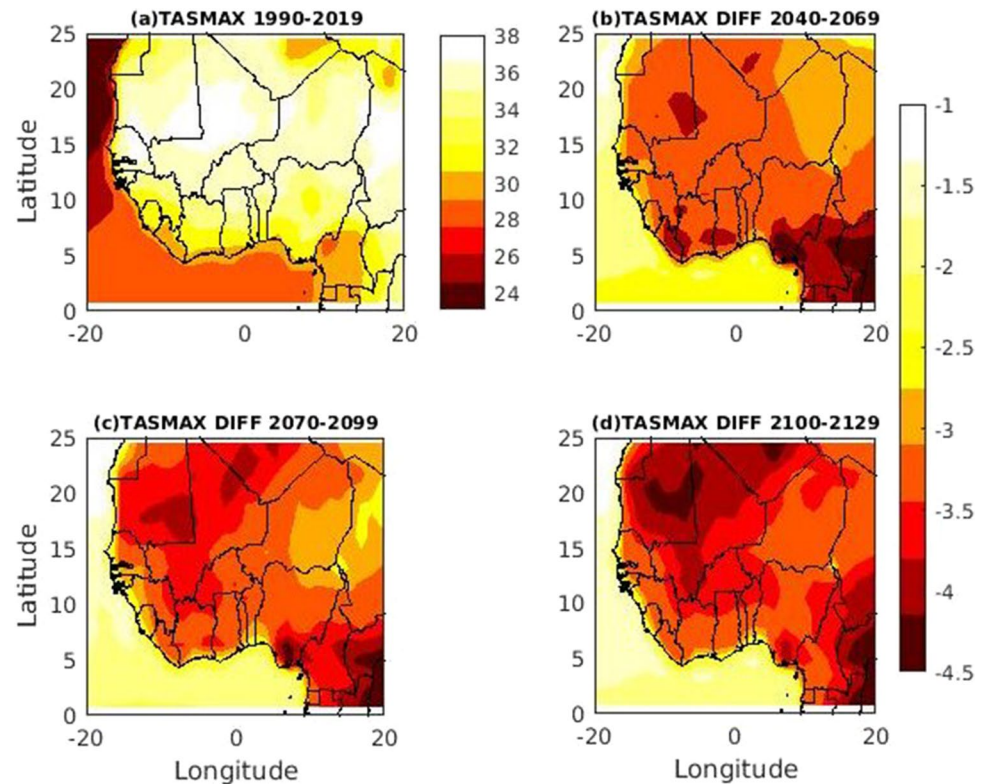
There is a general decrease in value of TASMAX at the periods with respect to the reference period in both the Sahel and Guinea regions (Fig. 6). Warming in Mauritania and northern part of Mali will decrease by 2.2 °C, while within the lower Sahel region comprising the southern part of Mali, southern part of Niger and northern parts of Benin and Nigeria, warming will decrease by 1.5 °C on average.

Fig.7 The difference between the reference period (1990–2019) of TASMIN and the periods 2040–2069, 2070–2099 and 2100–2129 under 1% per year CO_2 decrease up to preindustrial level. **a** Is the reference period. **b–d** Are the projected differences, statistically significant at 5% level and represented by the long color bar

Fig. 8 The difference between the reference period (1990–2019) of TS and the periods 2040–2069, 2070–2099 and 2100–2129 under 1% per year CO_2 decrease up to preindustrial level. **a** Shows the reference period. **b–d** Show the projected differences, statistically significant at 5% level and represented by the long color bar
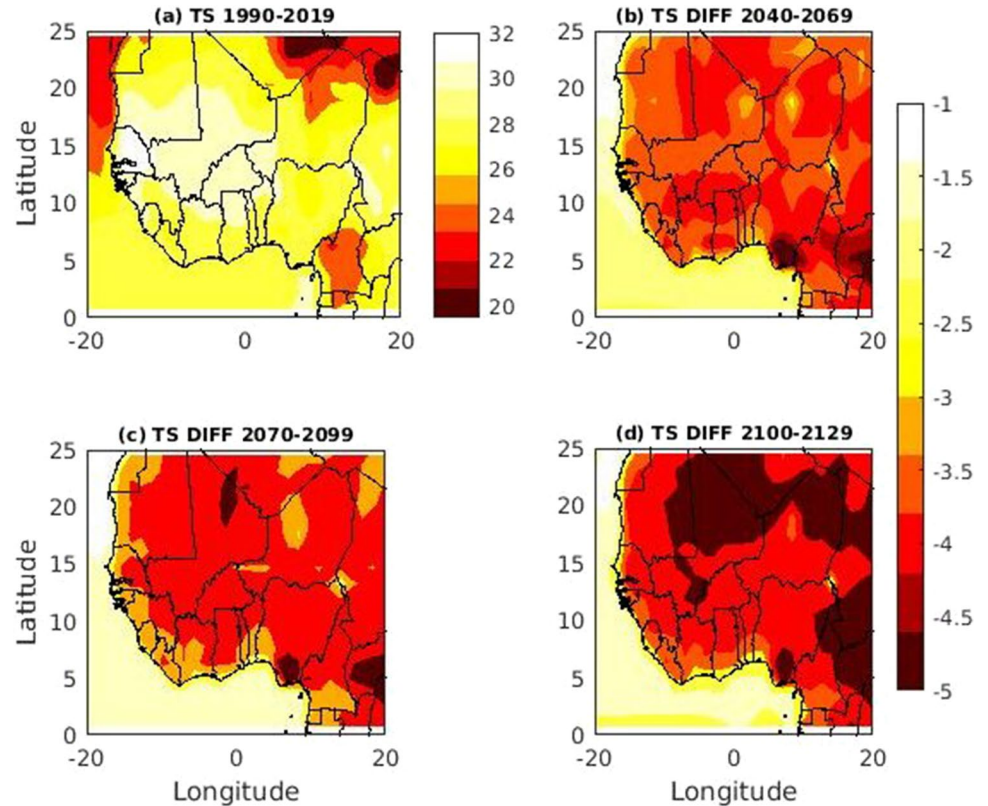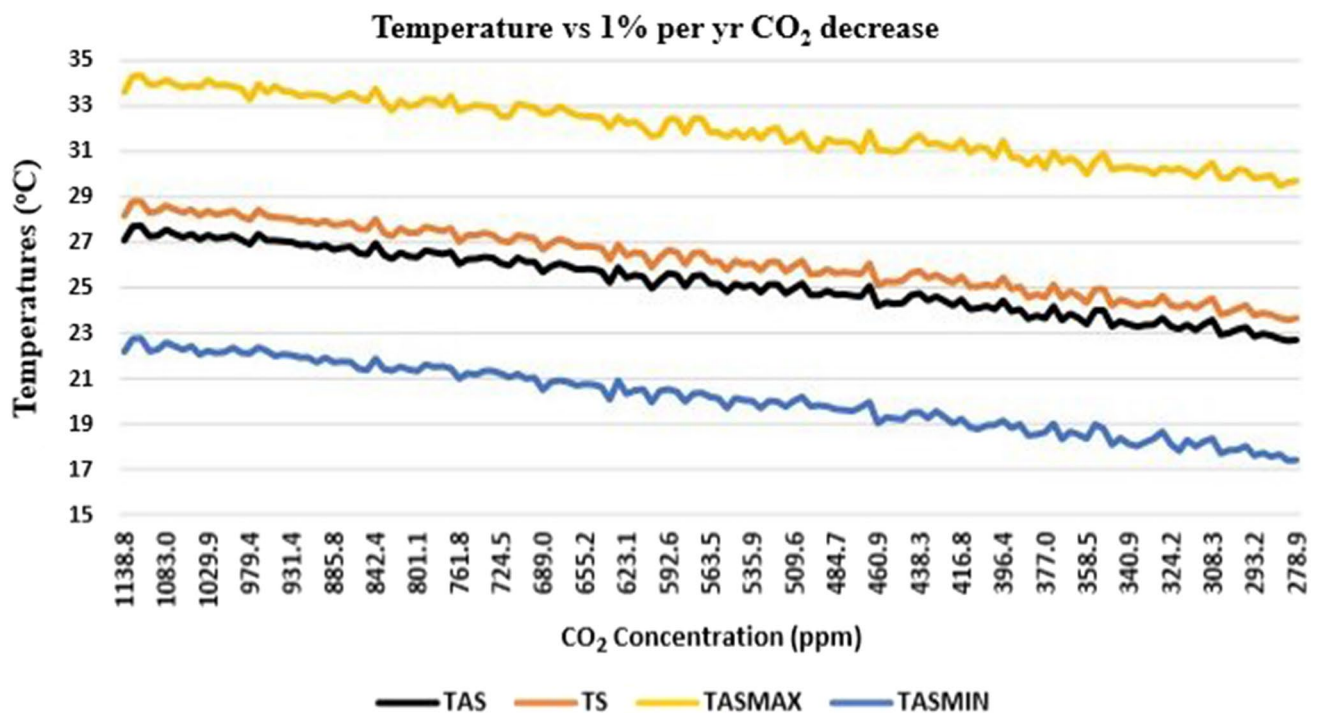
Fig. 9 The relationship between temperature and CO_2 concentration

Table 2 Maximum and minimum values of the parameters, the levels of co_2 removal impacts in the Sahel region indicated by the box red box in Fig. 10h

Parameters	Periods	Maximum (°C)	Minimum (°C)	Temperature change due to CDR (°C)
TAS	1990–2019	30.4 (16.5° N, 12° W, Mauritania)	22.8 (18.8° N, 9° E, Niger)	
	2040–2069	28.8 (17° N, 9° W, Mauritania)	21.2 (18.8° N, 9° E, Niger)	– 1.6
	2070–2099	27.6 (16.5° N, 12° W, Mauritania)	20.0 (18.8° N, 9° E, Niger)	– 2.8
	2100–2129	26.6 (15.1° N, 12° W, Mauritania)	18.6 (18.8° N, 9° E, Niger)	– 3.8
TASMAX	1990–2019	39.0 (16.5° N, 4° W, Mali)	34.4 (18.8° N, 9° E, Niger)	
	2040–2069	37.1 (17.5° N, 3° W, Mali)	32.9 (18.8° N, 9° E, Niger)	– 1.9
	2070–2099	36.0 (17.5° N, 3° W, Mali)	31.8 (18.8° N, 9° E, Niger)	– 3.0
	2100–2129	35.0 (17.5° N, 3° W, Mali)	30.5 (18° N, 9° E, Niger)	– 4.0
TASMIN	1990–2019	23.2 (15° N, 13° W, Senegal)	14.8 (18.8° N, 9° E, Niger)	
	2040–2069	21.4 (15° N, 13° W, Senegal)	13.0 (18.8ºN,10ºE, Niger)	– 1.8
	2070–2099	20.6 (15° N, 13° W, Senegal)	11.8 (18.8° N, 10° E, Niger)	– 2.6
	2100–2129	19.8 (15° N, 13° W, Senegal)	11.0 (18.8° N, 10° E, Niger)	–3.4
TS	1990–2019	33.0 (15.5° N, 13° W, Senegal)	23.8 (18.8° N, 9° E, Niger)	
	2040–2069	31.0 (15.5° N, 13° W, Senegal)	22.2 (18.8° N, 9° E, Niger)	– 2.0
	2070–2099	29.8 (15.5° N, 13° W, Senegal)	21.0 (18.8° N, 9° E, Niger)	– 3.2
	2100–2129	28.6 (15° N, 13° W, Senegal)	20.1 (18.8° N, 9° E, Niger)	– 4.4

Table 3 Maximum and minimum values of the parameters and the levels of CO_2 removal impacts in Guinea coast region indicated by the white box in Fig. 10h

Parameters	Periods	Maximum (°C)	Minimum (°C)	Temperature change due to CDR (°C)
TAS	1990–2019	29.6 (9° N, 1° W, Ghana))	25.0 (9° N, 9° E, Nigeria)	
	2040–2069	27.8 (9° N, 1° W, Ghana)	23.2 (9° N, 9° E, Nigeria)	− 1.8
	2070–2099	26.8 (9° N, 1° W, Ghana)	22.2 (9° N, 9° E, Nigeria)	− 2.8
	2100–2129	25.5 (9° N, 1° W, Ghana)	21.1 (9° N, 9° E, Ghana)	− 4.1
TASMAX	1990–2019	36.4 (9° N, 1° W, Ghana)	31.6 (7.8° N, 10° W, Liberia)	
	2040–2069	34.6 (9° N, 1° W, Ghana)	29.8 (7.8° N, 10° W, Liberia)	− 1.8
	2070–2099	33.8 (9° N, 1° W, Ghana)	29.0 (7.8° N, 10° W, Liberia)	− 2.6
	2100–2129	32.8 (9° N, 1° W, Ghana)	28.5 (7.8° N, 10° W, Liberia)	− 3.6
TASMIN	1990–2019	23.9 (9° N, 1° W, Ghana)	20.1 (9° N, 9° E, Nigeria)	
	2040–2069	21.7 (9° N, 1° W, Ghana)	18.1 (9° N, 9° E, Nigeria)	− 2.2
	2070–2099	20.6 (9° N, 1° W, Ghana)	17.0 (9° N, 9° E, Nigeria)	− 3.3
	2100–2129	19.5 (9° N, 1° W, Ghana)	16.1 (9° N, 9° E, Nigeria)	− 4.4
TS	1990–2019	31.6 (9° N, 1° W, Ghana)	26.4 (9° N, 9° E, Nigeria)	
	2040–2069	29.2 (9° N, 1° W, Ghana)	24.4 (9° N, 9° E, Nigeria)	− 2.4
	2070–2099	28.0 (9° N, 1° W, Ghana)	23.2 (9° N, 9° E, Nigeria)	− 3.6
	2100–2129	26.8 (9° N, 1° W, Ghana)	22.5 (9° N, 9° E, Nigeria)	− 4.8

The Guinea coast comprising Liberia, Cote D'Ivoire, Ghana, Togo, Benin, and southern part of Nigeria will record an average of 3.2 °C level of reduction in the parameter. In the period 2040–2069 (Fig. 6b), reduction of TASMAX around Sahel to the tune of 2.2 °C has been projected with respect to the reference period. TASMAX in the southern part of Nigeria involving Bayelsa, Delta, Rivers, Cross Rivers, Imo and Abia will be lowered by as much as 3.1 °C. The lowest values in TASMAX were projected in the western Sahel for the period, 2070–2099. The TASMIN will record the highest values on the average difference of 2.3 °C in the period, 2040–2069 (Fig. 7b). Much improvement in the reduction of the values of this parameter in the Sahel regions will be experienced during the 2070–2099 and 2100–2129 periods with much reduction level toward the northern part of Mali.

Decrease in surface temperature decreases evaporation and hence reduces dryness. According to UNHCR (2023), temperature in the Sahel is projected to rise between 2.0 and 4.3 °C by 2080, compared to preindustrial levels, with higher temperatures and more temperature extremes projected for the northern part of the region. However, the finding in this work show that with carbon dioxide removal, locations in the northern part of Mali and Niger, in particular, where higher decreases in temperature are projected will experience greater amount of wetness than other parts of Sahel in general. Usually, most parts of Senegal, The Gambia, Burkina Faso, southern part of Mali, Niger and the northern part of Nigeria are known for semi-arid warm tropical climate. As temperature reduces due to carbon dioxide removal, warming and heat waves are expected to reduce in these locations. In Guigma et al. (2020), most of the regions in the Sahel experience on average one or two heat waves per year with a duration of 3–5d and severe magnitude, as eastern Sahel experiences more frequent and longer events. Heat advection and the greenhouse effect of moisture are the main drivers of Sahelian heat waves. Heat waves are natural disasters often associated with an increase in daytime and/or nighttime temperatures (Ngoungue Langue et al. 2023). Contrary to this projection on the heat waves in Sahel, the simulated decrease in temperature is projected to have great positive impact in ameliorating heat waves related issues associated with eastern Sahel (Figs. 5d and 8d). Furthermore, improved temperature condition and wetness in Sahel will reduce herders–farmers conflict which usually ensues as herders migrate for animal grazing and home settlement in the region. For centuries, pastoralists have crossed the Sahel following seasonal patterns, which allowed them to feed their herds. The scarcity of water, pasture and fertile soil force people to migrate. Such displacement can lead to conflicts over land and resources between herders and farmers, which in turn further fuel displacement dynamics (International Displacement Monitoring Center 2020).

TS recorded a maximum and minimum values of 31.0 °C (in Senegal) and 22.2 °C (in Niger), respectively, for the period, 2040–2069 within Sahel. Its maximum and minimum values of 29.2 °C (in Ghana) and 24.4 °C (in Nigeria) were, respectively, simulated for Guinea coast. Higher values within this period are found from latitude 10° N and above comprising the Sahel region while lower ones are below the latitude, that is, the Guinea coast area. Subsequent periods–2070–2099 and 2100–2129 decreased proportionately

with the previous period to an average reduction of 3.5 °C and 4.2 °C, respectively, in Sahel and 2.8 °C and 3.9 °C, respectively, in the Guinea coast with respect to the reference period. As a major factor to indicate the degree of climate change, rise in TS induces warming. Therefore, locations with higher values of TS such as the Guinea locations at lower latitude in the period 2040–2069 (Fig. 8b) will be dry, but with a lower intensity compared with the intensity at the reference period, while locations with lower values will be slightly wetter than it was at the reference period. Sub-humid-warm tropics are found in Guinea, the southern part of Burkina Faso and Nigeria, while the southern parts of Guinea and Nigeria have a humid-warm tropical climate.

According to IPCC (2021), global warming scenarios over West Africa is projected at 1.5 °C, 1.5 °C and 1.4 °C for the periods 2021–2040 (near term), 2041–2060 (medium term) and 2081–2100 (long term), respectively, under a net zero carbon dioxide emission by 2050. Under high emission scenarios, warming for the same periods is projected at 1.6 °C, 2.4 °C and 4.4 °C, respectively. Comparatively, carbon dioxide removal simulation projected an average of 2.2 °C, 3.4 °C and 4.6 °C reductions in warming for the periods 2040–2069, 2070–2099 and 2100–2129, respectively. West African ecosystems are very sensitive to climate change and climate variability. This means that growth of natural vegetation across Africa will improve while desertification, biodiversity loss and species extinction engendered by warming climate are expected to recuperate. Lack of water availability is a serious issue in West Africa. Declining rainfall and increasing temperature, drought frequency and water demand have been identified as major causes of drying water bodies. Decrease in temperature with CO_2 removal will improve water availability for sustainable agricultural practices and hydropower purposes and reduce wild fire occurrence and land degradation. Decreased temperatures over West Africa due to atmospheric carbon dioxide removal has the potential to reduce the rate of occurrence of drought and its intensity. This minimizes the risk of disruption associated with wetlands and riverine systems with a resultant improvement in structural changes in plant and animal populations.

3.3 Time of retreat

The analysis of time of retreat (ToR as demonstrated in Figs. 10, 11, 12) to 2 °C level of reduction shows that, with TAS, under the threshold of signal-to-noise ratio $S/N < -1$, the retreat was projected by the year 2095 during autumn with a reduction of up to 2.2 °C (Table 4) in Sahel region, while it was captured in Guinea coast region by the year 2089 during summer with a reduction of up to 2.4 °C. Therefore, under the threshold of $S/N < -1$, ToR is simulated by

TAS from the year 2095 (autumn season) to 2107 (winter season) in Sahel and from the year 2089 (summer) to 2099 (winter season) in Guinea coast. In Sahel, with the threshold value of $S/N < -2$, ToR is expected in the year 2114 during autumn with an impact of -2.7 °C while in Guinea region, it is expected earlier in the year 2107 during autumn with maximum reduction 2.8 °C. Under the threshold of $S/N < -2$, ToR is simulated by TAS from the year 2114 (autumn season) to 2119 (winter season) in Sahel and from the year 2107 (autumn) to the year 2116 (winter season) in Guinea coast.

With TS, under the threshold of $S/N < -1$, the retreat was simulated by the year 2095 during autumn with a reduction of up to 2.1 °C in the Sahel region, while it was projected in the Guinea coast region by the year 2091 during summer with a reduction of up to 2.2 °C. Under this threshold, ToR is simulated by TS from the year 2095 (autumn season) to 2107 (winter season) in Sahel and from the year 2091 (autumn season) to 2109 (winter season) in Guinea coast. In Sahel, with the threshold value of $S/N < -2$, ToR is expected in the year 2115 during autumn with an impact of -2.6 °C, while in the Guinea region, it is expected earlier in the year 2111 during autumn with maximum reduction of 2.7 °C. Therefore, under this threshold, ToR is simulated by TS from the year 2115 (autumn season) to the year 2119 (winter season) in Sahel and from the year 2111 (autumn) to the year 2116 (winter season) in Guinea coast.

4 Conclusion

Over West Africa, temperature projection with CDRMIP declined toward the last period 2100–2129. Improvement in the level of wetness is expected with a significant reduction in temperature within the Sahel region before the end of the year 2100. Time of retreat to 2.0 °C reduction target is expected to occur much earlier during autumn and later during winter seasons. Furthermore, the time of retreat is simulated to occur earlier in the Guinea coast region with greater levels of impact than in the Sahel region and will occur mostly during the autumn season in both regions. Generally, the temperature of the atmosphere over West Africa is projected to reduce by at least 1.0 °C in 2040–2069 period, 1.7 °C in 2070–2099 period and 2.8 °C in the 2100–2129 period. Further work is therefore recommended to be done to study the impact of carbon dioxide removal in agriculture, heat stress and fire index over West Africa.

Fig.10 Median ToR for TAS. Column 1: **a** winter season (DJF), **c** spring season (MAM), **e** summer season (JJA) and **g** autumn season (SON) when temperature is expected to retreat to preindustrial level under a threshold value ToR < − 1. Column 2: **b** winter season (DJF), **d** spring season (MAM), **f** summer season (JJA) and **h** autumn season (SON) when temperature is expected to retreat to preindustrial level under a threshold value ToR < −2. The regions indicated by the red and white boxes are used in Fig. 12
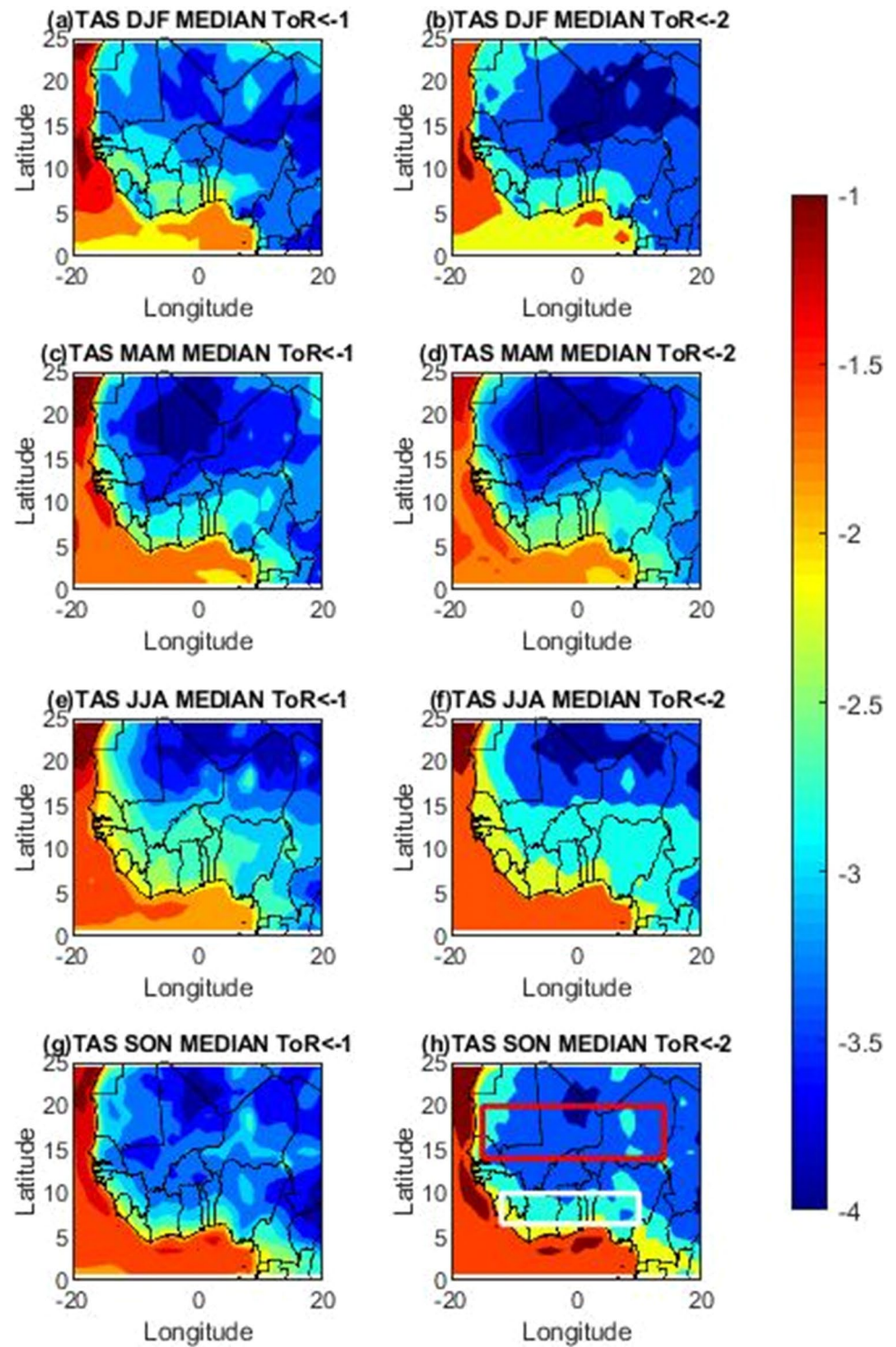
Fig. 11 Median ToR for TS. Column 1: **a** Winter Season (DJF), **c** Spring Season (MAM), **e** Summer Season (JJA) and **g** Autumn Season (SON) when temperature is expected to retreat to preindustrial level under a threshold value ToR < − 1. Column 2: **b** Winter Season (DJF), **d** Spring Season (MAM), **f** Summer Season (JJA) and **h** Autumn Season (SON) when temperature is expected to retreat to preindustrial level under a threshold value ToR < − 2
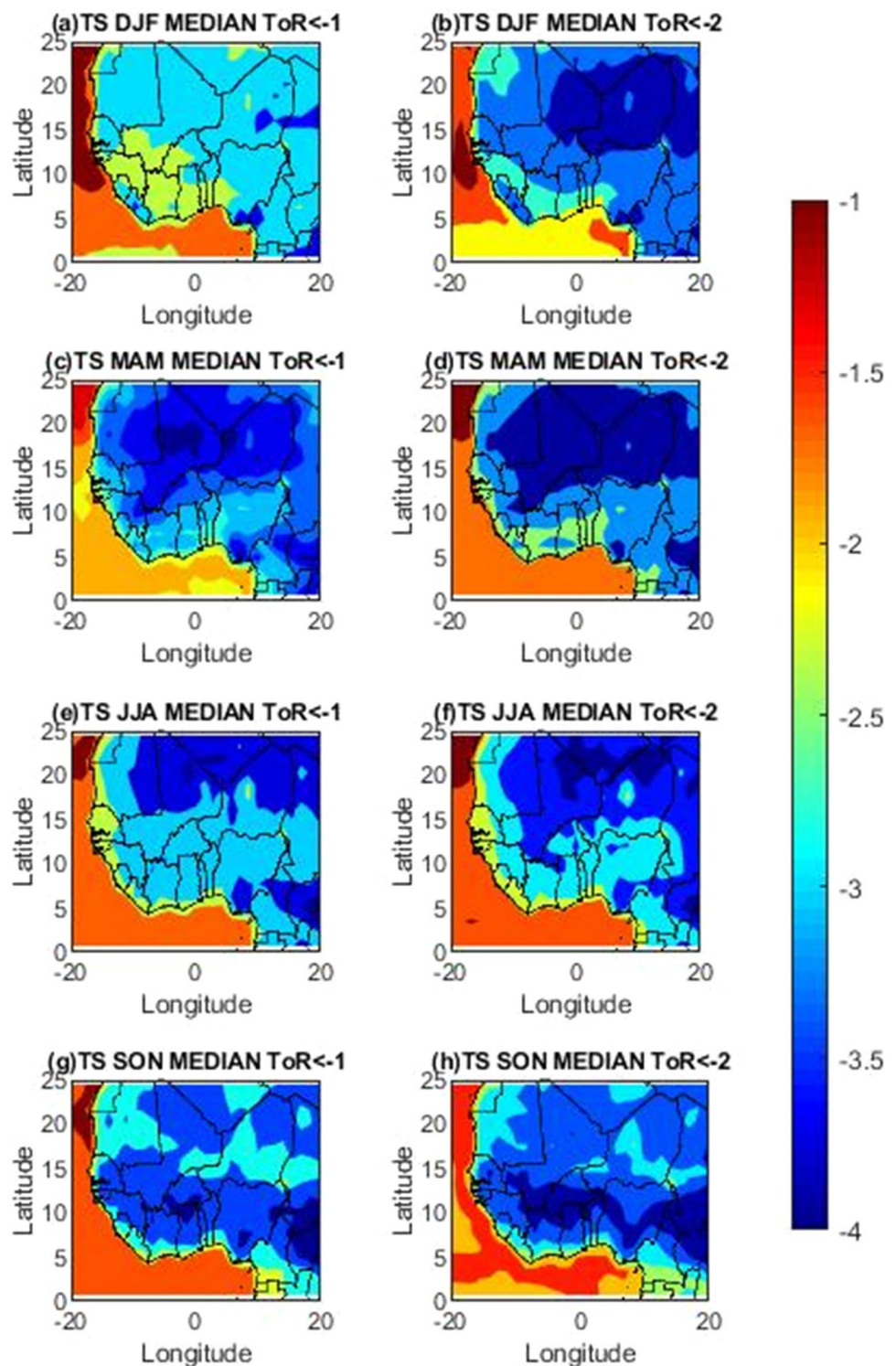
Fig. 12 Histograms representing the number of S/N < −2 temperature threshold in each decade. Column 1 is for the Sahel region indicated by the red box in Fig. 10h. **a** Seasonal plot for TAS and **c** seasonal plot for TS. Column 2 is for Guinea coast region indicated by the white box in Fig. 10h. **b** Seasonal plot for TAS and **d** seasonal plot for TS
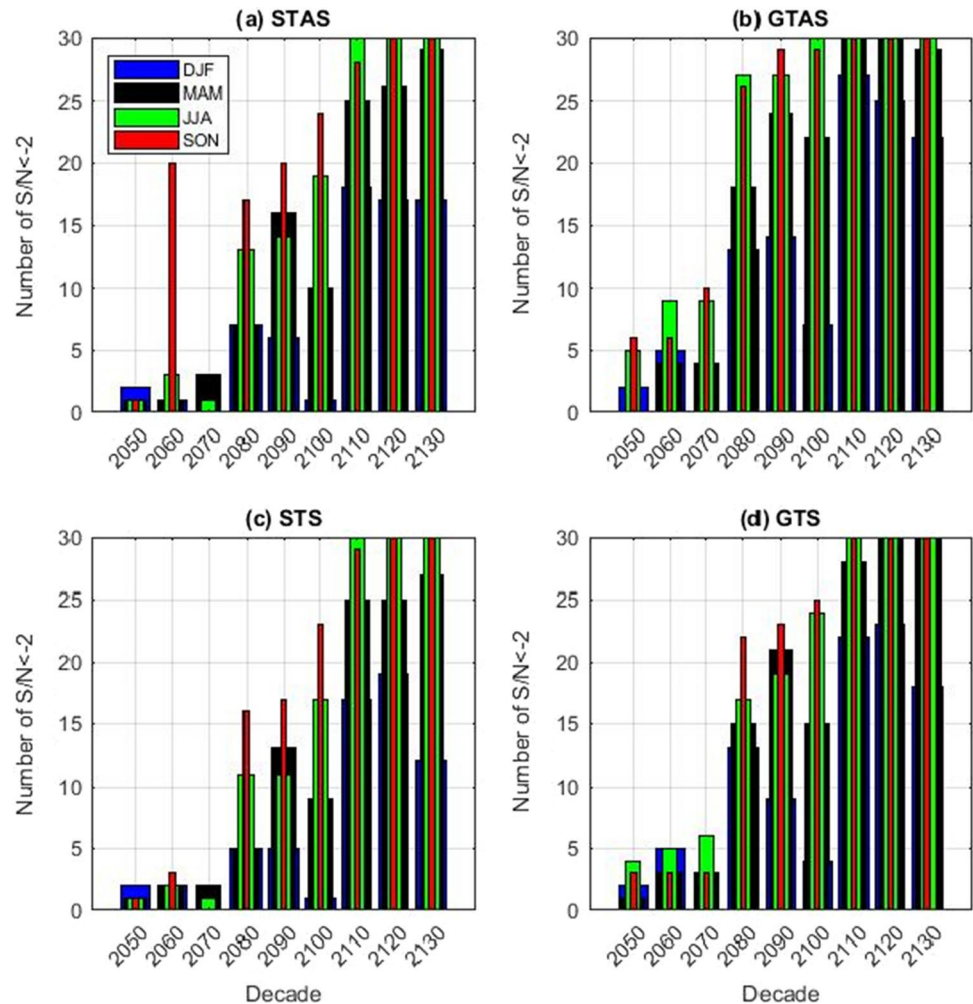
Table 4 Time of retreat under threshold values S/N < − 1 and S/N < − 2 for the two regions indicated by the red and white boxes in Fig. 10h

| | Seasons | SAHEL | | GUINEA | |
		Time of retreat < − 1 (°C)	Time of retreat < − 2 (°C)	Time of retreat < − 1 (°C)	Time of retreat < − 2 (°C)
TAS	Winter (DJF)	2107 (− 1.9)	2119 (− 2.4)	2099 (− 2.0)	2116 (− 2.6)
	Spring (MAM)	2096 (− 1.9)	2118 (− 2.6)	2090 (− 2.1)	2112 (− 2.7)
	Summer (JJA)	2096 (− 2.1)	2116 (− 2.6)	2089 (− 2.4)	2107 (− 2.8)
	Autumn (SON)	2095 (− 2.2)	2114 (− 2.7)	2090 (− 2.4)	2107 (− 2.8)
TS	Winter (DJF)	2107 (− 1.8)	2119 (− 2.5)	2102 (− 1.9)	2116 (− 2.5)
	Spring (MAM)	2097 (− 1.9)	2118 (− 2.5)	2093 (− 2.1)	2115 (− 2.6)
	Summer (JJA)	2096 (− 2.1)	2117 (− 2.6)	2091 (− 2.2)	2112 (− 2.7)
	Autumn (SON)	2095 (− 2.1)	2115 (− 2.6)	2091 (− 2.2)	2111 (− 2.7)

Numbers in parenthesis indicate the levels of impact for the corresponding year of retreat

References

Almazroui M, Saeed F, Saeed S et al (2020) Projected Change in Temperature and Precipitation Over Africa from CMIP6. Earth Syst Environ 4:455–475. https://doi.org/10.1007/s41748-020-00161-x

Borchers M, Thrän D, Chi Y, Dahmen N, Dittmeyer R, Dolch T, Dold C, Förster J, Herbst M, Heß D, Kalhori A, Koop-Jakobsen K, Li Z, Mengis N, Reusch TBH, Rhoden I, Sachs T, Schmidt-Hattenberger C, Stevenson A, Thoni T, Wu J, Yeates C (2022) Scoping carbon dioxide removal options for Germany-What is their potential contribution to Net-Zero CO2? Clim, Front. https://doi.org/10.3389/fclim.2022.810343

Chiang PC, Pan SY (2017) CO$_2$ Mineralization and Utilization via Accelerated Carbonation. In: Carbon Dioxide Mineralization and Utilization', Springer, Singapore https://doi.org/10.1007/978-981-10-3268-4_3.

Clarke L, Jiang K, Akimoto K, Babiker M, Blanford G, Fisher-Vanden K, Hourcade JC, Krey V, Kriegler E, Löschel A, McCollum D, Paltsev S, Rose S, Shukla PR, Tavoni M, Van der Zwaan B, Van Vuuren D (2014) Assessing Transformation Pathways. In: Climate Change 2014: Mitigation of Climate Change. Contribution of Working Group III to the Fifth Assessment Report of the Intergovernmental Panel on Climate Change Cambridge and New York: *Cambridge University Press.*

CRS (2022) Carbon Capture and Sequestration (CCS) in the United States. https://crsreports.congress.gov, R44902.

Deme AG, Amadou T, HOURDIN F (2017) Chapter 3. Climate projections in West Africa: the obvious and the uncertain In: Rural societies in the face of climatic and environmental changes in West Africa [online]. Marseille: IRD Éditions https://doi.org/10.4000/books.irdeditions.12325

Diallo I, Sylla MB, Giorgi F, Gaye AT, Camara M (2012) Multi-model GCM-RCM ensemble-based projections of temperature and precipitation over West Africa for the early 21st Century. International Journal of Geophysics 2012:972896. https://doi.org/10.1155/2012/972896

Diffenbaugh NS, Giorgi F (2012) Climate change hotspots in the CMIP5 global climate model ensemble. Clim Change 114(3–4):813–822

Eyring V, Bony S, Meehl GA, Senior CA, Stevens B, Stouffer RJ, Taylor KE (2016) Overview of the Coupled Model Intercomparison Project Phase 6 (CMIP6) experimental design and organization. Geosci Model Dev 9:1937–1958. https://doi.org/10.5194/gmd-9-1937-2016

Fitzpatrick RGJ, Parker DJ, Marsham JH et al (2020) How a typical West African day in the future-climate compares with current-climate conditions in a convection-permitting and parameterised convection climate model. Clim Change 163:267–296. https://doi.org/10.1007/s10584-020-02881-5

Flato G, Marotzke J, Abiodun B, Braconnot P, Chou SC, Collins W, Cox P, Driouech F,Emori S, Eyring V, Forest C, Gleckler P, Guilyardi E, Jakob B, Kattsov V, Reason C, Rummukainen M (2013) Evaluation of Climate Models. In: Climate Change 2013: The Physical Science Basis. Contribution of Working Group I to the Fifth Assessment Report of the Intergovernmental Panel on Climate Change [Stocker, T.F., D. Qin, G.-K. Plattner, M. Tignor, S.K. Allen, J. Boschung, A. Nauels, Y. Xia, V. Bex and P.M. Midgley (eds.)]. Cambridge University Press, Cambridge, United Kingdom and New York, NY, USA.

Fontaine B, Roucou P, Monerie PA (2011) Changes in the African monsoon region at medium-term time horizon using 12 AR4 coupled models under the A1B emissions scenario. Atmospheric Science Letters 12(1):83–88

Fuss S, Canadell JG, Peters GP, Tavoni M, Andrew RM, Ciais P, Jackson RB, Jones CD, Kraxner F, Nakicenovic N, Le Quere C, Raupach MR, Sharifi A, Smith P, Yamagata Y (2014) Betting on negative emissions' *Nature Clim*. Change 4(10):850–853

Griscom BW, Adams J, Ellis P, Houghton RA, Lomax G, Miteva DA, Schlesinger WH, Shoch D, Siikamäki J, Woodbury P, Zganjar C, Blackman A, Campari J, Conant RT, Delgado C, Elias P, Hamsik M, Kiesecker J, Landis E, Polasky S, Potapov P, Putz FE, Sanderman J, Silvius M, Smith P, Wollenberg E, Fargione J (2017) Natural pathways to climate mitigation' Proceedings of the National Academy of Sciences, USA (in press).

Guigma KH, Todd M, Wang Y (2020) Characteristics and thermodynamics of Sahelian heatwaves analysed using various thermal indices. Clim Dynam 55:3151–3175. https://doi.org/10.1007/s00382-020-05438-5,a,b,c,d

Harris NL, Gibbs DA, Baccini A et al (2021) Global maps of twenty-first century forest carbon fluxes. Nat Clim Chang 11:234–240. https://doi.org/10.1038/s41558-020-00976-6

Harris IC, Jones PD, Osborn T (2020) CRU TS4.04: Climatic Research Unit (CRU) Time-Series (TS) version 4.04 of high-resolution gridded data of month-by-month variation in climate (Jan. 1901-Dec. 2019). Centre for Environmental Data Analysis, *date of citation*. https://catalogue.ceda.ac.uk/uuid/89e1e34ec3554dc98594a5732622bce9

Hawkins E, Sutton R (2011) Time of emergence of climate signals', GEOPHYSICAL RESEARCH LETTERS, "*in press*", https://doi.org/10.1029/2011GL050087.

IPCC (2021) Climate Change 2021: The physical science basis. Contribution of working group I to the sixth assessment report of the intergovernmental panel on climate change

IPCC (2013) Warming of the climate system is unequivocal, and since the 1950s, many of the observed changes are unprecedented over decades to millennia. The atmosphere and ocean have warmed, the amounts of snow and ice have diminished, sea level has risen, and the concentrations of greenhouse gases have increased

Internal Displacement Monitoring Centre (2020) Global Report on Internal Displacement," Geneva, 2020. [Online]. Available: https://www.internal-displacement.org/publications/2020-global-report-on-internal-displacement

Keller DP, Lenton A, Littleton EW, Oschlies A, Scott V (2018) Vaughan NE (2018) The Effects of Carbon Dioxide Removal on the Carbon Cycle'. Springer, Current Climate Change Reports 4:250–265. https://doi.org/10.1007/s40641-018-0104-3

Kemper J (2015) Biomass and carbon dioxide capture and storage: a review'. Int J Greenh Gas Control 40:401–430. https://doi.org/10.1016/j.ijggc.2015.06.012

Lackner KS, Wendt CH, Butt DP, Joyce EL, Sharp DH (1995) Carbon dioxide disposal in carbonate minerals'. Energy 11(20):1153–1170

MacDougall AH (2013) Reversing climate warming by artificial atmospheric carbon-dioxide removal: can a Holocene-like climate be restored? Geophys Res Lett 40:5480–5485. https://doi.org/10.1002/2013GL057467

Mariotti L, Coppola E, Sylla MB, Giorgi F, Piani C (2011) Regional-climate model simulation of projected 21st century climate change over an all-Africa domain: comparison analysis of nested and driving model results. J Geophys Res D: Atmos 116(D15):D15111. https://doi.org/10.1029/2010JD015068

Marshall C (2017) In Switzerland, a giant new machine is sucking carbon directly from the air. Science, E&e News. https://doi.org/10.1126/science.aan6915

McLaren D (2012) A comparative global assessment of potential negative emissions technologies'. Spec Issue Negat Emiss Technol 90:489–500. https://doi.org/10.1016/j.psep.2012.10.005

Meehl GA, Covey C, Delworth T, Latif M, McAvaney B, Mitchell JFB, Stouffer RJ, Taylor KE (2007) The WCRP CMIP3 multimodel

dataset: a new era in climatic change research. Bull Am Meteor Soc 88(9):1383–1394

Miranda B, Stefan S, Matthias H, Sean L, Mark GL (2017) Carbon Dioxide Removal', IASS fAct Sheet 1/2017. Institute for Advanced Sustainability Studies (IASS) Potsdam, October 2017. https://doi.org/10.2312/iass.2017.017.

Monerie PA, Fontaine B, Roucou P (2012) Expected future changes in the African monsoon between 2030 and 2070 using some CMIP3 and CMIP5 models under a medium-low RCP scenario. J Geophys Res D: Atmos 117(16):D16111. https://doi.org/10.1029/2012JD017510

Mora CF, Frazier AG, Longman RJ, Dacks RS, Walton MM, Tong EJ, Sanchez JJ, Kaiser LR, Stender YO, Anderson JM, Ambrosino CM, Fernandez-Silva I, Giuseffi LM, Giambelluca TW (2013) The projected timing of climate departure from recent variability. Nature 502:183–187

Morrill JC, Bales RC, Conklin MH (2001) The relationship between air temperature and stream temperature', *American Geophysical Union.* (https://ui.adsabs.harvard.edu/abs/2001AGUSM...H42A09M/abstract).

Ngoungue Langue CG, Lavaysse C, Vrac M, Flamant C (2023) (2023) Heat wave monitoring over West African cities: uncertainties, characterization and recent trends. Nat Hazards Earth Syst Sci 23:1313–1333. https://doi.org/10.5194/nhess-23-1313-2023

Niang I et al (2015) 'Africa', Climate change 2014: Impacts, adaptation and vulnerability: Part B: regional aspects: working group II contribution to the fifth assessment report of the intergovernmental panel on climate change 1199–1266 https://doi.org/10.1017/cbo9781107415386.002

Niang, I., O.C. Ruppel, M.A. Abdrabo, A. Essel, C. Lennard, J. Padgham, and P. Urquhart (2014) Africa. In: Climate Change 2014: Impacts, Adaptation, and Vulnerability. Part B: Regional Aspects. Contribution of Working Group II to the Fifth Assessment Report of the Intergovernmental Panel on Climate Change [Barros, V.R., C.B. Field, D.J. Dokken, M.D. Mastrandrea, K.J. Mach, T.E. Bilir, M. Chatterjee, K.L. Ebi, Y.O. Estrada, R.C. Genova, B. Girma, E.S. Kissel, A.N. Levy, S. MacCracken, P.R. Mastrandrea, and L.L.White (eds.)]. Cambridge University Press, Cambridge, United Kingdom and New York, NY, USA, pp. 1199–1265.

Patricola CM, Cook KH (2010) Northern African climate at the end of the twenty-first century: an integrated application of regional and global climate models. Clim Dyn 35(1):193–212

Patricola CM, Cook KH (2011) Sub-Saharan Northern African climate at the end of the twenty-first century: forcing factors and climate change processes. Clim Dyn 37(5–6):1165–1188

Renforth P, Henderson G (2017) Assessing ocean alkalinity for carbon sequestration'. Reviews in Geophysics. https://doi.org/10.1002/2016RG000533

Shepard D (2019) Global warming: severe consequences for Africa; United Nations Africa Renewal. https://www.un.org/africarenewal/magazine/december-2018-march-2019/global-warming-severe-consequences-africa

Smith P, Davis SJ, Creutzig F, Fuss S, Minx J, Gabrielle B, Kato E, Jackson RB, Cowie A, Kriegler E, van Vuuren DP, Rogelj J, Ciais P, Milne J, Canadell JG, McCollum D, Peters G, Andrew R, Krey V, Shrestha G, Friedlingstein P, Gasser T, Grübler A, Heidug WK, Jonas M, Jones CD, Kraxner F, Littleton E, Lowe J, Moreira JR, Nakicenovic N, Obersteiner M, Patwardhan A, Rogner M, Rubin E, Sharifi A, Torvanger A, Yamagata Y, Edmonds J, Yongsung C (2016) Biophysical and economic limits to negative CO_2 emissions'. Nat Clim Chang 6:42–50. https://doi.org/10.1038/nclimate2870

UNFCCC (2015) Adoption of The Paris Agreement FCCC/CO/2015/L.9/Rev.1 http://unfccc.int/resource/docs/2015/cop21/eng/l09r01.pd.

UNHCR (2023) Representative Concentration Pathways - Climate Risk Profile Sahel region https://www.unhcr.org/my/media/39788

USNAS (2015) Climate Intervention: Carbon Dioxide Removal and Reliable Sequestration', US National Academy of Sciences, Washington D.C.

van Vuuren DP, Deetman S, van Vliet J, van den Berg M, van Ruijven BJ, Koelbl B (2013) The role of negative CO2 emissions for reaching 2°C—insights from integrated assessment modelling'. Clim Change 118(1):15–27

Vizy EK, Cook KH, Crétat J, Neupane N (2013) Projections of a wetter Sahel in the twenty-first century from global and regional models. J Clim 26(13):4664–4687

Woolf D, Amonette JE, Street-Perrott A, Lehmann J, Joseph S (2010) Sustainable biochar to mitigate global climate change', Nature Communications 1. Article. https://doi.org/10.1038/ncomms1053

Zedler JB, Kercher S (2005) Wetland resources: status, trends, ecosystem services, and restorability'. Annu Rev Environ Resour 30:39–74

Ziehmann C (2000) Comparison of a single-model EPS with a multi-model ensemble consisting of a few operational models'. Tellus a: Dynamic Meteorology and Oceanography 52(3):280–299. https://doi.org/10.3402/tellusa.v52i3.12266